1-1-2015

3D MR Ventricle Segmentation in Pre-term Infants with Post-Hemorrhagic Ventricle Dilation

Wu Qiu
Western University, wqiu@robarts.ca

Jing Yuan
Western University

Jessica Kishimoto
Western University

Yimin Chen
City University of Hong Kong

PROCEEDINGS OF SPIE

SPIEDigitalLibrary.org/conference-proceedings-of-spie

3D MR ventricle segmentation in pre-term infants with post-hemorrhagic ventricle dilation

Wu Qiu
Jing Yuan
Jessica Kishimoto
Yimin Chen
Sandrine de Ribaupierre
Bernard Chiu
Aaron Fenster

SPIE.

3D MR Ventricle Segmentation in Pre-term Infants with Post-Hemorrhagic Ventricle Dilation

Wu Qiu[a], Jing Yuan[a], Jessica Kishimoto[a], Yimin Chen[b], Sandrine de Ribaupierre[c], Bernard Chiu[b], and Aaron Fenster[a]

[a]Robarts Research Institute, University of Western Ontario, London, Ontario, Canada.
[b]Department of Electronic Engineering, City University of Hong Kong, China.
[c]Neurosurgery, Department of Clinical Neurological Sciences, University of Western Ontario, London, Ontario, Canada.

ABSTRACT

Intraventricular hemorrhage (IVH) or bleed within the brain is a common condition among pre-term infants that occurs in very low birth weight preterm neonates. The prognosis is further worsened by the development of progressive ventricular dilatation, i.e., post-hemorrhagic ventricle dilation (PHVD), which occurs in 10-30% of IVH patients. In practice, predicting PHVD accurately and determining if that specific patient with ventricular dilatation requires the ability to measure accurately ventricular volume. While monitoring of PHVD in infants is typically done by repeated US and not MRI, once the patient has been treated, the follow-up over the lifetime of the patient is done by MRI. While manual segmentation is still seen as a gold standard, it is extremely time consuming, and therefore not feasible in a clinical context, and it also has a large inter- and intra-observer variability. This paper proposes an segmentation algorithm to extract the cerebral ventricles from 3D T1-weighted MR images of pre-term infants with PHVD. The proposed segmentation algorithm makes use of the convex optimization technique combined with the learned priors of image intensities and label probabilistic map, which is built from a multi-atlas registration scheme. The leave-one-out cross validation using 7 PHVD patient T1 weighted MR images showed that the proposed method yielded a mean DSC of $89.7\% \pm 4.2\%$, a MAD of 2.6 ± 1.1 mm, a MAXD of 17.8 ± 6.2 mm, and a VD of $11.6\% \pm 5.9\%$, suggesting a good agreement with manual segmentations.

Keywords: Ventricle Segmentation, Pre-term Neonate with PHVD, Convex Optimization, Multi-Atlas Initialization, 3D MR Imaging.

1. INTRODUCTION

Ventriculomegaly is a common condition in neonates born prematurely with the highest risk population being those born at < 32 weeks gestation or with very low birth weight (< 1500 g). Intraventricular hemorrhage (IVH) is one of the primary non-congenital causes of ventriculomegaly, which is brain bleeding that occurs in 15 to 30% of very low birth weight preterm neonates.[1] Infants with IVH are at risk of developing progressive dilatation of the ventricles, a pathology called hydrocephalus. Ultrasound (US) or MR images of their brains are typically used to monitor the ventricular size.[2–6] The treatment is surgical, involving, for example, the placement of a shunt, where a tube is surgically inserted to divert cerebral spinal fluid (CSF) from the ventricles to abdomen in order to decrease pressure on the surrounding brain. Once the patient is treated, the efficiency of the treatment is evaluated by MRI, and the patients are typically followed with regular MRI over their lifetime to assess the good functioning of the shunt. Should a shunt become blocked, the ventricles would increase in size, necessitating a surgical revision to replace the shunt. Currently the ventricular volume is estimated by measureing the width and shape of the ventricles on orthogonal planes; however access to an accurate volume would simplify the decision algorithm of the clinician. While clinicians have a good sense of what ventriculomegaly looks like compared to normal ventricles, it is difficult to determine small changes in ventricle size, as can happen in patient treated with a shunt. As discussed below, neonatal imaging, especially in IVH patients imposes some technical challenges; and manual segmentation is too labour intensive to be used in a clinical context. This paper proposes a segmentation algorithm to extract the cerebral ventricles from 3D T1-weighted MR images of pre-term infants with PHVD.

Wu Qiu (Corresponding author), E-mail: wqiu@robarts.ca. Address: Imaging Research Laboratories, Robarts Research Institute, University of Western Ontario, P.O. Box 5015, 100 Perth Drive, London, Ontario, Canada, N6A 5K8.

Medical Imaging 2015: Image Processing, edited by Sébastien Ourselin, Martin A. Styner, Proc. of SPIE Vol. 9413, 941310 · © 2015 SPIE · CCC code: 1605-7422/15/$18 · doi: 10.1117/12.2081467

Previous brain segmentation algorithms have been extensively investigated in adult brain MR images.[7] However, there is limited publicly available software for neonatal brain MR image segmentation, and none have been developed to account for the extensive deformation of the ventricles caused by hydrocephalus. Neonatal brain MR images tend to suffer from high image noise (the patients are not sedated and therefore the images have some additional motion artefacts), low tissue contrast, and considerable inter-subject anatomical variability, making most of the methods used in adult population not applicable to these images.[8] Although some automatic neonatal MR segmentation methods were developed,[9–11] most of works segmented neonatal brain in MR images into white matter (WM), gray matter (GM), and CSF, and did not focus on the ventricular system. Moreover, their methods were only validated on healthy neonate images. A population of IVH patients adds another challenge, as the hemorrhage leads to an heterogeneous cerebrospinal fluid (CSF) as well as sometimes the development of periventricular cysts. Therefore, a large inter-subject anatomical variability is possible, and overtime, as the brain develops, an intra-individual variability is also possible. Because most clinical images are performed in a 1.5T, trying to minimize the time needed to acquire an image, the resolution of the images is relatively poor.

2. NEW OR BREAKTHROUGH WORK TO BE PRESENTED

In this study, we propose an atlas initialized multi-region segmentation method for extracting the cerebral ventricles from 3D T1 weighted (T1w) MR images of pre-term PHVD neonate patients. The proposed algorithm makes use of convex optimization technique combined with multi-atlas registration framework and multi-region constraints. The major components of the whole segmentation pipeline are implemented using general-purpose programming on graphics processing units (GPGPU) to obtain a high computational efficiency. Note that this work has not been submitted for any publication or presentation elsewhere.

3. METHODS

3.1 Segmentation overview

All images are bias corrected using the N3 algorithm,[12] and subsequently head masked via the BET algorithm.[13] The head mask is only used to locate the position of the head, and the segmentation is carried out without skull-stripping to avoid potential over-stripping of the head. Each training image of $(I_i(x),\ i = 1, 2, ..., n)$ is registered by $\mathbf{u}_i^{affine}(x)$ to the subject image $I_s(x)$ using an affine block-matching approach with default parameters, which is implemented in the Nifty Reg package.[14] Following the affine registration, a recently developed novel deformable registration algorithm (TV-Reg)[15,16] is used to efficiently and accurately extract the non-linear registration $\mathbf{u}_i^{non-linear}(x)$, $i = 1, 2, ..., n$, from each pre-segmented image I_i to the subject image I_s. Specially, it makes use of a coarse-to-fine strategy to capture the large deformations and employs an efficient multiplier-based algorithm to compute the updated incremental deformation field at each image scale.

The multiple registered labels are combined via a weighting strategy to acquire the probabilistic labeling map, which is used as the shape prior for the subsequent segmentation step. A thresholding procedure follows to generate the initial guess for the ventricles and to approximate the intensity appearance priors, i.e. the probability density functions (PDFs), for the background and foreground ventricle regions respectively.

3.2 Deformable registration algorithm (TV-Reg)

we use a multi-scale dual optimization-based method[15,16] to estimate the non-linear deformation field $\mathbf{u}(x) = [\mathbf{u}_1(x), \mathbf{u}_2(x), \mathbf{u}_3(x)]^T$, between two given images $I_1(x)$ and $I_2(x)$, which minimizes a variational optical-flow energy function, i.e.

$$\min_u \ \ P(I_1, I_2; \mathbf{u}) \ + \ R(\mathbf{u}) \tag{1}$$

where $P(I_1, I_2; u)$ represents a dissimilarity measure of the two input images $I_1(x)$ and $I_2(x)$ under deformation by $\mathbf{u}$, and $R(\mathbf{u})$ is the regularization function to match a deformation field with the required smoothness. In this paper, we employ the sum of absolute intensity differences (SAD):

$$\min_u \ \ P(I_1, I_2; \mathbf{u}) \ := \ \int_\Omega |I_1(x + \mathbf{u}) - I_2(x)| \ dx \, , \tag{2}$$

as an effective and robust similarity measurement to the two input images from the same imaging modalities.

The L_p-norm convex function as the regularization term is used in this work, such that:

$$R(\mathbf{u}) := \alpha \sum_{i=1}^{3} \int_{\Omega} |\nabla \mathbf{u}_i|^p \, dx \tag{3}$$

where $p \geq 1$. In this study, $p = 1$, which gives rise to a non-smooth function, specifically the sum of three convex total-variation functions: $R(\mathbf{u}) = \alpha \int_{\Omega}(|\nabla \mathbf{u}_1| + |\nabla \mathbf{u}_2| + |\nabla \mathbf{u}_3|)dx$.

Because of the expected non-linearity and non-convexity of the image functions $I_1(x)$ and $I_2(x)$, it is challenging to directly optimize the energy function (1), even if its regularization term $R(u)$ is convex. To address this issue, we introduce an incremental linearization and convexification approach to solving the studied optimization problem (1), which lends itself to a standard coarse-to-fine optimization framework. This approach allows for a global-optimization perspective, properly avoiding local optima through the ability to capture large deformations.[15,16]

3.3 Segmentation problem formulation

A convex optimization-based method is finally used to obtain the globally optimal segmentation of the given 3D image $I(x)$ into the foreground ventricle region $\mathbb{R}$ and background $\Omega \backslash \mathbb{R}$, which encodes the prior information obtained in the multi-atlas initialization procedure and minimizes the total labeling cost joint with the total area of $\mathbb{R}$, i.e., the continuous min-cut problem,[17] such that

$$\min_{\mathbb{R}} \quad \int_{\mathbb{R}} D_F(x)\, dx \, + \int_{\Omega \backslash \mathbb{R}} D_B(x)\, dx \, + \int_{\partial \mathbb{R}} ds \tag{4}$$

Typically, the minimization of total area of the segmented regions consists of finding a smooth bounded surface of the ventricle region $\mathbb{R}$. In this study, the two cost functions $D_F(x)$ and $D_B(x)$ in (4) measure the fidelity of each pixel fitting the respective prior models, i.e.:

$$D_F(x) \, = \, -\alpha \log F(I(x)) \, - (1-\alpha) \log \big(P_L(x) * G_\sigma(x)\big) \tag{5}$$

and

$$D_B(x) \, = \, -\alpha \log B(I(x)) \, - (1-\alpha) \log \big(1 - P_L(x) * G_\sigma(x)\big)\,, \tag{6}$$

where the first term measures the intensity similarity of each voxel compared with the sampled voxels in the ventricle region and the background region by the log-likelihood of the respective intensity PDFs;[18] the second term measures the similarity extent of each voxel to the shape prior model by the log-likelihood of the probabilistic shape prior map $P_L(x)$; $\alpha \in (0,1)$ weights the contributions from the intensity and shape priors for each voxel. In Eq. 5 and 6, $G_\sigma(x)$ is the Gaussian smoothing function.

3.4 Convex optimization and continuous max-flow algorithm

We denote $u(x)$ as the indicator function of the estimated region $\mathbb{R}$ such that

$$u(x) := \begin{cases} 1\,, & \text{where } x \text{ is inside } \mathbb{R} \\ 0\,, & \text{otherwise} \end{cases} \quad , \quad i = f : foreground, b : background\,. \tag{7}$$

The indicator functions $u(x) \in \{0,1\}$, for $\forall x \in \Omega$, are also called the labeling functions.

Therefore, the proposed optimization model (4) can be equally reformulated as the *continuous min-cut model*:

$$\min_{u(x)\in[0,1]} \, \langle 1-u, D_F(x)\rangle + \langle u, D_B(x)\rangle + \int_{\Omega} g(x)\, |\nabla u| \, dx\,, \tag{8}$$

where the binary constraints $u(x) \in \{0,1\}$ are substituted instead of its convex relaxation $u(x) \in [0,1]$. The minimization of eq. 8 can be solved globally and exactly by an efficient continuous max-flow algorithm.[17]

Table 1. Segmentation results of 7 PHVD patients' T1w MR images regarding DSC, MAD, MAXD, and VD, represented as Mean ± SD.

DSC (%)	MAD (mm)	MAXD (mm)	VD (%)
89.75 ± 4.2	2.6 ± 1.1	17.8 ± 6.2	11.6 ± 5.9

More specifically, we use a continuous max-flow configuration[17,19–21] in this study. Let $p_s(x)$ and $p_t(x)$ be source and sink flows to and from pixel x to the source and sink terminals. The spatial flow $p(x)$ exists around the neighborhood of pixel x. Then, the continuous max-flow model that maximizes the flow can be formulated as follows:

$$\max_{p_s,p_t,p} \int_\Omega p_s(x)\, dx \tag{9}$$

subject to the flow capacity and conservation conditions.

$$\begin{cases} p_s(x) \le C_s(x), & \forall \in \Omega \\ p_t(x) \le C_t(x), & \forall \in \Omega \\ |p(x)| \le g(x), \ \forall \in \Omega \end{cases} \tag{10}$$

and the flow conservation condition:

$$\mathrm{div}\,(p(x) - p_s(x) + p_t(x)) = 0, \ \forall \in \Omega \tag{11}$$

It has been proven that the continuous max-flow model (9) is equivalent to the convex relaxation problem (8).[17] The continuous max-flow model (9) is then formulated and solved using the classical augmented Lagrangian method.[22] The readers are referred to [17,23] for more details about the continuous min-cut/max-flow method.

4. RESULTS

Seven preterm-born patients with PHVD were imaged upon reaching term-equivalent age with a 1.5T Signa HDxt MRI scanner (General Electric Health Care, Milwaukee, WI) without sedation. A 3D T1-weighted (T1w) MR image of each brain was acquired while the patient was bundled inside a MedVac blanket (CFI Medical Solutions Inc, Fenton, MI). The leave-one-out cross validation strategy was used to evaluate the proposed approach. A manual segmentation of each image used as the ground truth was compared to the algorithm segmented result, using *volume-based metrics*: Dice similarity coefficient (DSC); *distance-based metrics*: the mean absolute surface distance (MAD) and maximum absolute surface distance (MAXD); and *volume measurement metrics*:absolute volume difference (VD), $|(V_{Manual} - V_{algorithm})/V_{Manual}|$.

Figure 1 shows an example of the algorithm segmented ventricle of one PHVD patient, visually demonstrating a good agreement. Table 1 shows the mean quantitative segmentation results for 7 patient images using the proposed method.Computations were carried out on a Tesla C2070 GPU (NVIDIA, St. Clara, CA) with an Ubuntu 12.04 machine and 144 GB RAM, where each computation of convex optimization required approximately 35 seconds. Each pairwise registration from one training image to the target subject was made up of an affine registration (no GPU acceleration: 3 minutes) and deformable registration (GPU: 50 seconds). Thus, leave-one-out cross validation using 7 images required an average of 24 miniutes for each subject image using 6 training atlas images.

5. CONCLUSIONS

PHVD is a common condition among pre-term IVH infants. Predicting PHVD accurately and determining if that specific patient with ventricular dilatation requires the ability to measure accurately ventricular volume. This paper proposes an approach to extract the brain ventricles of 3D T1 weighted (T1w) MR images of pre-term PHVD neonatal patients. The proposed segmentation algorithm makes use of the convex optimization technique combined with a label probabilistic shape prior, built via a multi-atlas non-linear registration scheme. The leave-one-out cross validation show that the proposed method is accurate and efficient, capable of capturing the large inter-subject shape variability. The generated DSCs along with MAD, MAXD, and VD are favourable in clinical practice, suggesting the proposed method could be potentially used to measure the ventricle system volume of the PHVD neonatal brain.

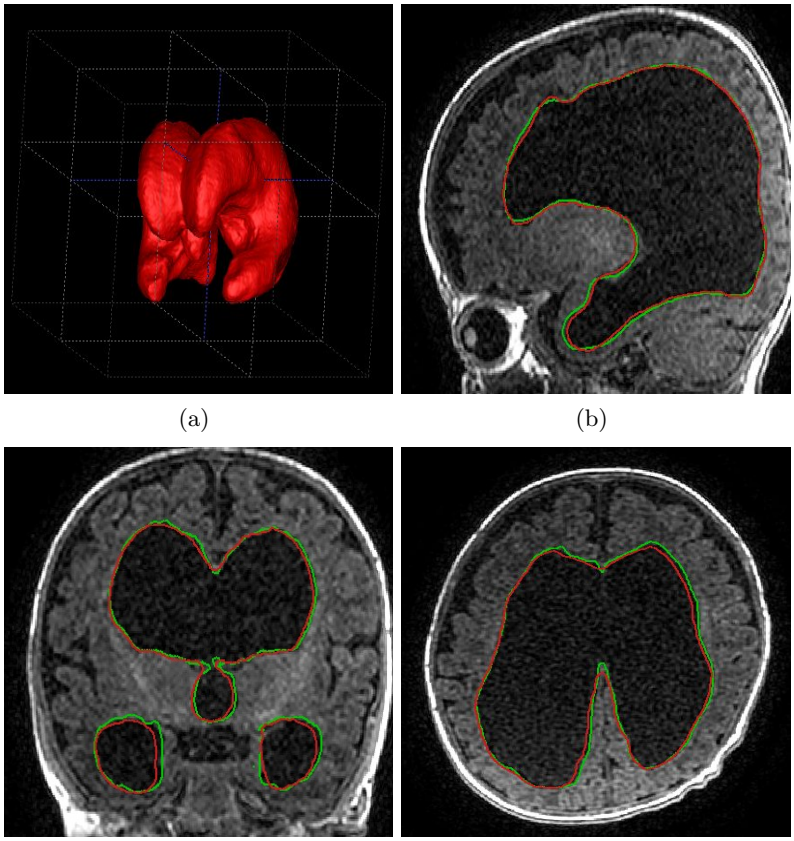

(a) (b) (c) (d)

Figure 1. Segmented ventricles colored in red compared to manual segmentation colored in green, DSC: 92.3%. (a)-(b): segmented surface, sagittal view, coronal view, and transverse view.

Acknowledgments

The authors are grateful for the funding support from the Canadian Institutes of Health Research (CIHR), Academic Medical Organization of Southwestern Ontario (AMOSO), the Research Grant Council of the HKSAR, China (Project No. CityU 139713), and the National Natural Science Foundation of China (Grant No. 81201149).

REFERENCES

[1] Synnes, A. R., Chien, L.-Y., Peliowski, A., Baboolal, R., and Lee, S. K., "Variations in intraventricular hemorrhage incidence rates among canadian neonatal intensive care units," *The journal of pediatrics* **138**(4), 525–531 (2001).

[2] Gilmore, J. H., Gerig, G., Specter, B., Charles, H. C., Wilber, J. S., Hertzberg, B. S., and Kliewer, M. A., "Infant cerebral ventricle volume: a comparison of 3-d ultrasound and magnetic resonance imaging," *Ultrasound in medicine & biology* **27**(8), 1143–1146 (2001).

[3] Kishimoto, J., de Ribaupierre, S., Lee, D., Mehta, R., St Lawrence, K., and Fenster, A., "3D ultrasound system to investigate intraventricular hemorrhage in preterm neonates," *Physics in medicine and biology* **58**(21), 7513 (2013).

[4] Qiu, W., Yuan, J., Kishimoto, J., Ukwatta, E., and Fenster, A., "Lateral ventricle segmentation of 3D pre-term neonates US using convex optimization," *MICCAI* (2013).

[5] Qiu, W., Yuan, J., Kishimoto, J., de Ribaupierre, S., Ukwatta, E., and Fenster, A., "Semi-automatic segmentation of pre-term neonate ventricle system from 3D ultrasound images," *IEEE International Symposium on Biomedical Imaging (ISBI)* (2014).

[6] Qiu, W., Yuan, J., Kishimoto, J., McLeod, J., de Ribaupierre, S., and Fenster, A., "User-guided segmentation of preterm neonate ventricular system from 3d ultrasound images using convex optimization," *Ultrasound in Medicine & Biology* **41**(2), 542–556 (2015).

[7] Ashburner, J. and Friston, K. J., "Unified segmentation," *NeuroImage* **26**(3), 839–851 (2005).

[8] Gui, L., Lisowski, R., Faundez, T., Hüppi, P. S., Lazeyras, F., and Kocher, M., "Morphology-driven automatic segmentation of MR images of the neonatal brain," *Medical image analysis* **16**(8), 1565–1579 (2012).

[9] Wang, L., Shi, F., Lin, W., Gilmore, J. H., and Shen, D., "Automatic segmentation of neonatal images using convex optimization and coupled level sets," *NeuroImage* **58**(3), 805–817 (2011).

[10] Wang, L., Shi, F., Li, G., Gao, Y., Lin, W., Gilmore, J. H., and Shen, D., "Segmentation of neonatal brain MR images using patch-driven level sets," *NeuroImage* **84**(0), 141 – 158 (2014).

[11] Shi, F., Fan, Y., Tang, S., Gilmore, J. H., Lin, W., and Shen, D., "Neonatal brain image segmentation in longitudinal MRI studies," *NeuroImage* **49**(1), 391–400 (2010).

[12] Sled, J. G., Zijdenbos, A. P., and Evans, A. C., "A nonparametric method for automatic correction of intensity nonuniformity in MRI data," *IEEE Trans. Med. Imag.* **17**(1), 87–97 (1998).

[13] Smith, S. M., "Fast robust automated brain extraction," *Human brain mapping* **17**(3), 143–155 (2002).

[14] Ourselin, S., Stefanescu, R., and Pennec, X., "Robust registration of multi-modal images: towards real-time clinical applications," *Medical Image Computing and Computer-Assisted Intervention (MICCAI)* , 140–147 (2002).

[15] Sun, Y., Yuan, J., Rajchl, M., Qiu, W., and Fenster, A., "Efficient convex optimization approach to 3D non-rigid MR-TRUS registration," *Medical Image Computing and Computer-Assisted Intervention (MICCAI)* (2013).

[16] Rajchl, M., Baxter, J. S., Qiu, W., Khan, A. R., Fenster, A., Peters, T. M., and Yuan, J., "Rancor: Non-linear image registration with total variation regularization," *arXiv preprint arXiv:1404.2571* (2014).

[17] Yuan, J., Bae, E., and Tai, X., "A study on continuous max-flow and min-cut approaches," *CVPR* (2010).

[18] Boykov, Y. and Funka-Lea, G., "Graph cuts and efficient N-D image segmentation," *International Journal of Computer Vision* **70**(2), 109–131 (2006).

[19] Qiu, W., Yuan, J., Ukwatta, E., Rajchl, M., yue sun, and Fenster, A., "Efficient 3D multi-region prostate MRI segmentation using dual optimization," *Information Processing in Medical Imaging (IPMI)* (2013).

[20] Qiu, W., Yuan, J., Ukwatta, E., Sun, Y., Rajchl, M., and Fenster, A., "Dual optimization based prostate zonal segmentation in 3D MR images," *Medical Image Analysis* **18**(4), 660–673 (2014).

[21] Qiu, W., Yuan, J., Ukwatta, E., Sun, Y., Rajchl, M., and Fenster, A., "Prostate segmentation: An efficient convex optimization approach with axial symmetry using 3D TRUS and MR images," *IEEE Trans. Med. Imag.* **33**(4), 947–960 (2014).

[22] Rockafellar, R. T., "Augmented Lagrangians and applications of the proximal point algorithm in convex programming," *Math. Oper. Res.* **1**(2), 97–116 (1976).

[23] Yuan, J., Bae, E., Tai, X.-C., and Boykov, Y., "A continuous max-flow approach to potts model," *ECCV* (2010).